ResearchGate

See discussions, stats, and author profiles for this publication at: https://www.researchgate.net/publication/325497740

Graft orientation influences meshing ratio

Article *in* Burns · May 2018

DOI: 10.1016/j.burns.2018.05.001

CITATIONS
0

READS
121

5 authors, including:

Lukas Capek
Technical University of Liberec
58 PUBLICATIONS **243** CITATIONS
SEE PROFILE

Cormac Flynn
Galway-Mayo Institute of Technology
38 PUBLICATIONS **517** CITATIONS
SEE PROFILE

Martin Molitor
Bulovka University Hospital
42 PUBLICATIONS **238** CITATIONS
SEE PROFILE

Petr Henyš
Technical University of Liberec
34 PUBLICATIONS **71** CITATIONS
SEE PROFILE

Some of the authors of this publication are also working on these related projects:

Measuring initial implant fixation by vibro - acoustic method View project

Improved Skin Graft Mesher View project

All content following this page was uploaded by Petr Henyš on 04 June 2018.

The user has requested enhancement of the downloaded file.

Can orientation of skin graft influence the meshing ratio?

Lukas Capek[a], Cormac Flynn [b], Martin Molitor [c], Simon Chong [d] and Petr Henys [a*],

[a] Technical University of Liberec, Department of Structure and Technologies, Studentska 2, 46117 Liberec 1, Czech Republic

[b] Waikato Institute of Technology, Private Bag 3036, Hamilton 3240, New Zealand

[c] University Hospital Bulovka, Department of Plastic Surgery, Budinova 8, Prague, Czech Republic

[d] Anglesea Hospital, Department of Plastic & Reconstructive surgery, 19 Knox St, Hamilton, New Zealand

Corresponding Author:

Petr Henys,
e-mail: petr.henys@tul.z

tel: +420485353257

fax: +420485353542

Total word count: 3517

Keywords: burn**,** finite element method, Langer line, biomechanics

Abstract

Objectives:

The technique of meshed skin grafting is known since 1960s. It was shown that there is a difference between the declared and real expansion ratio of the skin meshed graft. We hypothesize that the orientation of the Langer's lines in a split thickness skin graft is a key parameter in the resulting expansion ratio.

Methods:

The skin graft meshing process was analysed in two steps. In the first step, *ex vivo* uniaxial tests of human skin were performed. This served as an input for the constitutive model used for numerical simulations. In the second step, finite element analyses were performed so that stress distributions and expansion ratios could be determined.

Results:

It was shown that peaks of true stress tended to be concentrated around the vertex of the mesh pattern region for all cases. The declared expansion was impossible to obtain for all expansion ratios having the meshing incision perpendicular to the Langer´s lines. The highest difference between declared and real expansion ratio reaches 37 %.

Conclusions:

With regard to literature dealing with expansion of skin grafts by meshing, a high scatter amongst data results is observed. This finding was also explained by our research, demonstrating the significance of Langer's lines and their relative orientation to the direction of meshing.

1. Introduction

Split thickness skin grafting is a mainstay surgical technique for soft tissue reconstruction worldwide. In cases of large defects or limited donor site availability, the classic example being major burn injuries, skin grafts may be expanded beyond their original geometry. This permits a smaller graft to reconstruct a larger defect. Principally, there are two techniques used for skin expansion: tissue expansion, and skin graft meshing [1,2]. The first technique consists of overstretching the skin by gradual mechanical distention, usually in the form of a surgically inserted underlying silicone implant that is progressively expanded. This procedure is slow and usually takes several weeks, but allows skin to be expanded without significant attenuation of thickness [3]. The biomechanics of tissue expansion have also been studied through the use of computational models [4,5]. In contrast, meshing consists of the patterned placement of innumerable uniform short parallel incisions into a sheet of graft, usually through a specialized roller device. The incisions open upon application of perpendicular stretch, producing a regular pattern of rhomboid interstices. These two approaches therefore utilize fundamentally different biomechanical principles. The first creates new tissue through a slow, guided biological process, while the second one simply maximises the use of existing tissue through immediate mechanical means. While tissue expansion is well documented in the medical literature, there is a relative dearth of research on skin expansion through meshing.

The technique of meshed skin grafting was first introduced by Tanner et al. in 1964 [6,7]. While the original principles remain to this day, time and innovation have allowed modifications and refinements to the technique; variable expansion ratios can be achieved by utilizing longer incisions, while convenience has advanced through innovations such as electrical devices. Handerson et al. performed a detailed comparison of declared and real

expansion ratios [8]. While a large difference (up to 46 %) was found, they did not propose a specific reason for this difference. The clarification of this phenomena was not solved elsewhere [9,10].

Human skin is a stratified tissue with a highly nonlinear and anisotropic behavior, Langer´s lines correspond to the natural orientation of collagen fibers in the dermis and are generally parallel to the orientation of the underlying muscle fibers [11]. So that it is favorable to use this natural orientation in the following hypothesis. It is clear that skin graft orientation may play a role in the expansion achievable by meshing.

The following study introduces the dependency of skin mesh expansion ratio as a function of Langer´s lines orientation. We hypothesize that the orientation of the Langer's lines in a split thickness skin graft is a parameter playing a key role in the resulting expansion ratio.

2. Materials and methods

The skin graft meshing process was analysed in two steps. In the first step, *ex vivo* uniaxial tests of human skin were performed. This served as an input for the constitutive model used for numerical simulations. In the second step, finite element analyses were performed so that stress distributions and expansion ratios could be determined. The finite element method (FEM) is a standardized tool in biomechanics used for solving different tasks [12], and has been successfully used in the field of plastic and reconstructive surgery [13-16].

2.1 Ex vivo experiments

All the *ex vivo* experiments were carried out under ethical approval in accordance with Czech Republic laws and medical regulations. Skin was harvested from the discarded abdominoplasty specimen of a 44-year-old female. The skin graft was visually without any colour changes. The orientation of Langer's lines was recorded prior to graft harvest. The skin

was then manually tensioned to its original size, and eight rectangular grafts were harvested using a powered Dermatome (*Zimmer Czech, Czech Republic*) set. The grafts were planned to be 0.75 mm thick. Consistency of graft thickness was inspected using an optical microscope (*Nikon, Czech Republic*). The effective dimensions of the test specimens were 8 x 20 mm. Specimens were obtained in two orientations: parallel and perpendicular to the direction of the Langer´s lines, figure 1. Tensile tests were performed using a universal tensile test machine Testometric M350-5CT with 10 N force gauge. The samples were pre-tensioned by a force 0.1 N, and then tested to failure with a stretch rate of 20 mm/min.

Finite element models

The proposed computational model was based on the geometry of a standard skin graft mesher (*Zimmer Czech, Czech Republic*) with expansion ratios of 1.5:1, 2:1 and 3:1, and graft dimensions of 24 x 47 mm. The finite element model was created in the software MSC.Marc 2016.0 (*MSC.Software, Czech Republic*). The FEM mesh was created semi-automatically and was defined by four node planar elements (38 750 elements). The thickness of elements was 0.75mm. The slits were modelled by coincident nodes that were not connected, so that the free edges could open in the loading direction. The convergence error was minimized by using the adaptive mesh refinement Zienkiewitz-Zhu stress criterion in the location with the highest field gradient. The behaviour of the skin graft was assumed to be isotropic elastic and nonlinear [17]. The nonlinear elastic Yeoh phenomenological model was used [18]. The material constants for the constitutive law were estimated by using Matlab (*Humusoft Ltd., Czech Republic*), tab.1. The curve fit is shown on figure 2. The following boundary conditions were taken into consideration for numerical purposes, figure 3:

- The left edge of the domain was constrained kinematically in all degrees of freedom.

- Nodes corresponding to the right edge of the graft were connected via rigid body (RB) linked to a control node that was positioned further right.
- A displacement (X axis) of 36, 48 and 72 mm, corresponding to the theoretical declared directional expansion, was prescribed to the control node.
- In cases where the maximal true stress exceeded the ultimate strength of tested samples for declared expansions, the displacement of the control node was updated in such a way that the maximal true stress reached only 95 % of ultimate strength. The ultimate strength is the maximum stress that a material is capable of sustaining.

The models were loaded according to the above mentioned boundary conditions for grafts taken parallel and perpendicular to the Langer´s lines and for three different expansion ratios. After expanding the graft, the resultant overall meshed area was analysed by the software Geomagic (*Geomagic Ltd., USA*) and compared to the unexpanded graft geometry. Shrinkage was defined as the transversal maximal displacement measured according to figure 4. The distribution of true stress, shrinkage, expansion force, expanded surface and expansion ratio were calculated for each numerical model, corresponding to the different expansion ratios of the skin grafts.

3. Results

The mean thickness of skin samples gained in the parallel and perpendicular directions was in accordance with the setting on the skin graft mesher (0.75 mm). The measured stress-strain curves exhibited regular shapes for human soft tissues, with low stiffness for low stretch values, rapidly increasing stiffness with higher stretches, and a sudden stress decrease at failure [19]. Specimens meshed with incisions perpendicular to the Langer´s lines achieved up to 18.3 % higher extensibility than those oriented parallel to Langer’s lines.

The resultant values of true stress, shrinkage, expansion force, expanded surface and expansion ratio for each numerical model (corresponding to different expansion ratio of the skin graft) are summarized in Appendix (A1, A2 and A2). The resultant shape of the mesh interstices were either spindle shaped (1.5:1 and 2:1) or S-shaped (3:1). The peaks of true stress tended to be concentrated around the vertex of the mesh pattern region for all cases, figure 5. The maximal shrinkage was highest at 1.7 mm for 3:1 (declared expansion), and lowest at 0.3 mm for 1.5:1 (declared expansion). The expansion force for declared expansion was highest at 3.3 N for 3:1 and lowest at 0.3 N for 1.5:1.

For all expansion ratios, the declared expansion was impossible to obtain through stretching the graft in the X axis while having the meshing incision perpendicular to the Langer´s lines.

The maximal true stress exceeded the ultimate strength for all specimens with meshing incisions oriented perpendicular to Langer's lines. In other words, it would fail, table 2. The opposite was observed for those specimens meshed with incisions parallel to Langer's lines. For expansion ratios of 2:1 and 3:1, the true stress exceeded the ultimate strength of the skin. For expansion 1.5:1 the true stress was lower than ultimate strength. This meant that the declared expansion was reached. Having calculated the maximal expansion corresponding to ultimate strength (in both directions) the differences between declared and calculated expansions are demonstrated in figure 6.

4. Discussion

The use of skin graft meshing, with expansion ratios from 1.5:1 to 3:1, is common and routine in clinical practice (especially burns care). Faced with insufficient skin graft expansion, some technical modifications were proposed [20, 21]. The presence of Langers´s lines is well

known and widely applied in plastic and reconstructive surgery [22,23]. The dependency of skin behavior according to these lines has been proven by several authors [24-26]. Donor site availability is the ultimate factor limiting split thickness skin graft harvest quantity. Nevertheless, the local Langer's line orientation may explain the huge scatter in the expansion ratios achieved in practice. The technical expertise of the surgical practitioner may also play a significant role.

Our study demonstrated that the orientation of meshing incisions in a split thickness skin graft, relative to Langer´s lines, plays a crucial role in the achieved expansion ratios after meshing. The difference in declared and achieved expansion ratios according to the Langer´s lines orientation ranged from 0 % (1.5:1) up to 21 % (3:1). In general, greater expansion ratios were achieved when the applied stretch was perpendicular to the Langer's lines. This was due to such grafts exhibiting sufficient tensile strength to withstand expansion up to the specified ratio – we hypothesise that this strength was due to preservation of collagen integrity, in keeping with the underlying principle of Langer's lines.

The most detailed studies regarding skin expansion were performed by Lyons et al. and Kamolz et al. Lyons demonstrated that for all expansion ratios greater than 1:1, the extent of actual expansion was significantly less than that expected for each device [27]. Moreover, for larger expansion ratios, there were increasingly greater discrepancies between the area predicted by the device manufacturer and the actual area obtained in practice. Kamolz showed that skin meshers with ratios 1.5:1 and 3:1 did not achieve their claimed values (84.7% and 53.1% of the claimed expansion respectively).

When compared to these studies, our results were generally consistent. The finite element analyses demonstrated that the most loaded area of the expanded graft is the vertex of the mesh pattern. Lyons demonstrated that maximum graft areas obtained were less than the manufacturer's declared ratio by 11.28 % (1.5:1) and 22.81 % (3:1). Our results showed that

the range of error between the declared ratio and the FEM results was wider, depending on the orientation relative to Langer´s lines.

With regard to literature dealing with expansion of skin grafts by meshing, a high scatter amongst data results is observed. This finding was also explained by our research, demonstrating the significance of Langer's lines and their relative orientation to the direction of meshing. In this way, surgical technique with respect to both harvesting and meshing may strongly influence the resulting expansion ratio.

We recognize certain limitations of our methodology. Our conclusions derive from a skin grafts gained from a single donor, in the setting of elective abdominoplasty – the collagen may therefore have been subject to prior injury through pregnancy or obesity. Repeating our study with specimens from multiple patients may introduce a wider scatter in mechanical properties observed. This fact further aids the explanation of scatter in gained results after meshing the skin grafts. The computer model of the skin was assumed to be isotropic, which means the skin load response is independent on load direction. Both mentioned limits should be clarified.

Conflict of interest

There are no conflicts of interest.

References

[1] Gurtner G, Neliga P. Plastic surgery. New York: Elsevier; 2012.

[2] Kamolz LP, Lumenta D. Dermal Replacements in General, Burn, and Plastic Surgery. New York: Elsevier; 2013.

[3] Pasyk KA, Argenta LC, Austad ED. Histopathology of human expanded tissue. Clin

Plast Surg. 1987;14(3):435-45.

[4]Zollner A, Tepole AB, Gosain A, Kuhl E. Growing skin. Tissue expansion in pediatric forehead reconstruction. Biomech Model Mechanobiol. 2012 Jul; 11(6): 855–867.

[5] Pamplona D, Carvalho C. Characterization of human skin through skin expansion. J Mech Mat Struct. 2012;7:643-655.

[6] Tanner, J. C., Vandeput, J. and Olley, J. F. (1964). The mesh skin graft. Plastic and Reconstructive Surgery, 34, 287.

[7] Boudana D, Wolber A, Coeugniet E, Martinot-Duquennoy V, Pellerin P. History of skin graft. Ann Chir Plast Esthet. 2010;55(4):328-32.

[8] Henderson J, Arya R, Gillespie P. Skin graft meshing, over-meshing and cross-meshing. Int J Surg. 2012;10(9):547-50.

[9] Kamolz L, Schintler M, Parvizi D, Selig H, Lumenta D. The real expansion rate of meshers and micrografts: things we should keep in mind. Ann Burns Fire Disasters. 2013 Mar 31; 26(1): 26–29.

[10] Lyons JL, Kagan RJ. The true meshing ratio of skin graft meshers. J Burn Care Res. 2014 May-Jun;35(3):257-60.

[11] Agache A, Humbert P. Measuring the skin. London: Springer;2004.

[12] Holzapfel G, Ogden R. Biomechanics: Trends in Modelling and Simulation. Berlin: Springer; 2017.

[13] Akaishi S, Akimoto M, Ogawa R, Hyakusoku H. The relationship between keloid growth pattern and stretching tension: visual analysis using the finite element method. Ann Plast Surg. 2008;60(4):445-51.

[14] Limbert G. Mathematical and computational modelling of skin biophysics: a review. Proc Math Phys Eng Sci. 2017;473(2203):20170257.

[15] Buganza-Tepole A, Steinberg JP, Kuhl E, Gosain AK. Application of finite element modeling to optimize flap design with tissue expansion. Plast Reconstr Surg. 2014;134(4):785-92.

[16] Yoshida H, Tsutsumi S, Mizunuma M, Yanai A. A surgical simulation system of skin sutures using a three-dimensional finite element method. Clin Biomech. 2001;16(7):621-6.

[17] Bischoff JE, Arruda EM, Grosh K. Finite element modeling of human skin using an isotropic, nonlinear elastic constitutive model. J Biomech. 2000;33(6):645-52.

[18] Martins P, Jorge R, Ferreira R. A Comparative Study of Several Material Models for Prediction of Hyperelastic Properties: Application to Silicone-Rubber and Soft Tissues. 2006;42:135-147.

[19] Tong P, Fung YC. The stress-strain relationship for the skin. J Biomech. 1976;9(10):649-57.

[20] Henderson J, Arya R, Gillespie P. Skin graft meshing, over-meshing and cross-meshing. Int J Surg. 2012;10(9):547-50.

[21] Singh M, Nuutila K, Collins KC, Huang A. Evolution of skin grafting for treatment of burns: Reverdin pinch grafting to Tanner mesh grafting and beyond. Burns. 2017 Sep;43(6):1149-1154.

[22] Wilhelmi BJ, Blackwell SJ, Phillips LG. Langer's lines: to use or not to use. Plast Reconstr Surg. 1999;104(1):208-14.

[23] Waldorf JC, Perdikis G, Terkonda SP. Planning incisions. Oper Tech Gen Surg. 2002;4(3):199-206.

[24] Lanir, Y, Fung Y C. Two-dimensional mechanical properties of rabbit skin–ii. experimental results. J Biomech. 1974; 7(2):171–174.

[25] Bush J, Ferguson MW, Mason T, McGrouther G. The dynamic rotation of Langer's lines on facial expression. J Plast Reconstr Aesthet Surg. 2007;60(4):393-9.

[26] Ní Annaidh A, Bruyère K, Destrade M, Gilchrist MD, Otténio M. Characterization of the anisotropic mechanical properties of excised human skin. J Mech Behav Biomed Mater. 2012 ;5(1):139-48.

[27] Lyons JL, Kagan RJ. The true meshing ratio of skin graft meshers. J Burn Care Res. 2014;35(3):257-60.

Figures and table

Fig. 1. Orientation of skin samples according to Langer´s lines on abdomen

Fig. 2. Mathematical extrapolation of measured tensile tests of *ex vivo* skin

Fig. 3. Boundary conditions of finite element model

Fig. 4. Schema of meshed graft shrinkage measurement

Fig. 5. Location of true stress concentration around mesh interstices

Fig. 6. Differences between declared and calculated expansions ratios

Table 1. Material constants used for Yeoh nonlinear elastic model

Table 2. Binary comparative table of declared and computed expansions ratio: 💻📠🕑 - reached, :-(- not reached

Appendix

A1 – Summarized results for expansion rate 3:1

	Declared expansion parallel to LL	Max expansion parallel to LL	Declared expansion perpendicular to LL	Max expansion perpendicular to LL
Max true stress (MPa)	34.2	1.06	9.7	0.88

Expansion force (N)	3.3	2.7	2.9	1.4
Expanded surface (mm^2)	2933	2140	2843	2684
Shrinkage (mm)	1.7	1.1	1.4	0.9
Exp. ratio FEM	2.60	1.90	2.52	2.38
Result	Fail	No-fail	Fail	No-fail

A2 – Summarized results for expansion rate 2:1

	Declared expansion parallel to LL	**Max expansion parallel to LL**	**Declared expansion perpendicular to LL**	**Max expansion perpendicular to LL**
Max true stress (MPa)	14.6	1.06	2.7	0.88
Expansion force (N)	2.1	1.7	1.2	0.89
Expanded surface (mm^2)	2193	1762	2154	2080
Shrinkage (mm)	1.1	0.3	1.1	0.5
Exp ratio FEM	1.94	1.56	1.91	1.84
Result	Fail	No-fail	Fail	No-fail

A3 – Summarized results for expansion rate 1.5:1

	Declared expansion parallel to LL	**Max expansion parallel to LL**	**Declared expansion perpendicular to LL**	**Max expansion perpendicular to LL**
Max true stress (MPa)	9.7	1.06	0.3	-
Expansion force (N)	1.3	1.2	0.72	-
Expanded surface (mm^2)	1661	1566	1658	-
Shrinkage (mm)	0.4	0.3	0.5	-
Exp ratio FEM	1.47	1.38	1.47	-
Result	Fail	No-fail	No-fail	-

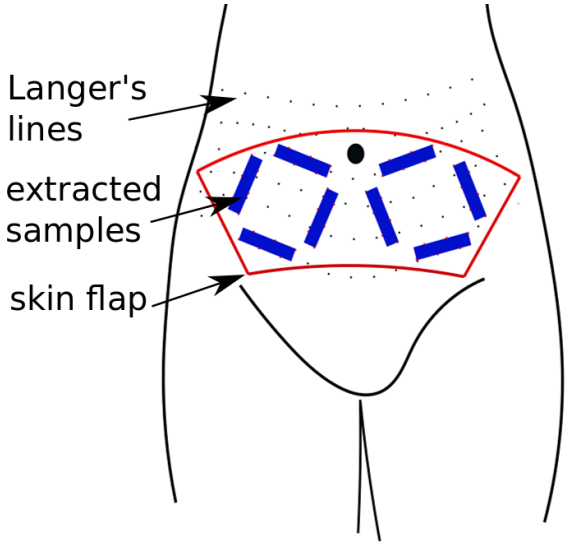

Fig.1

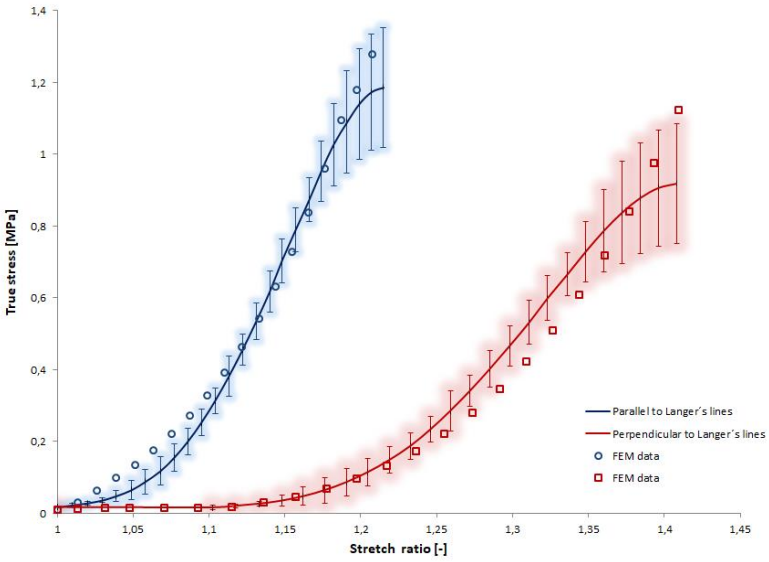

Fig.2

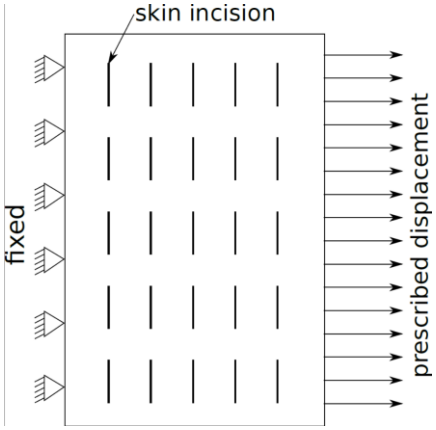

Fig.3

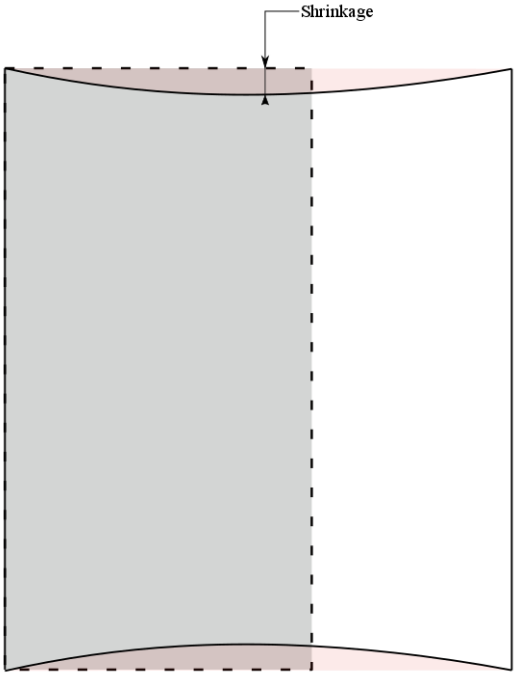

Fig.4

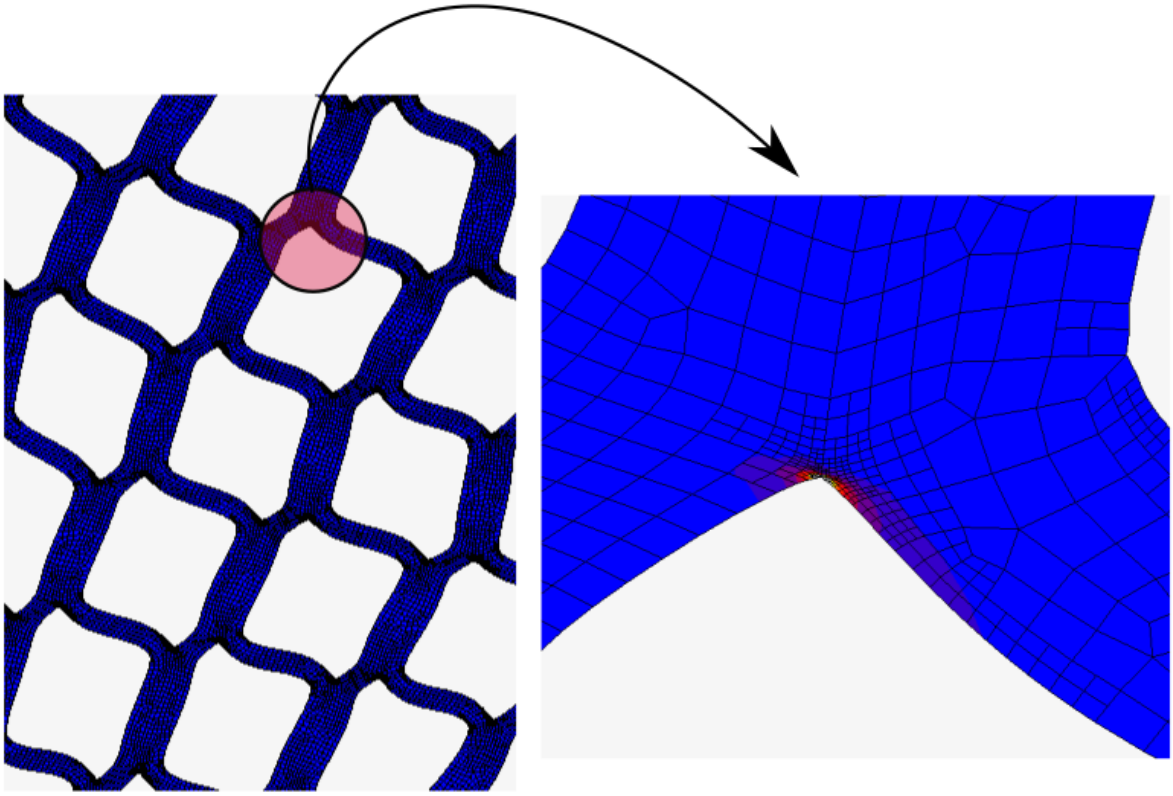

Fig.5

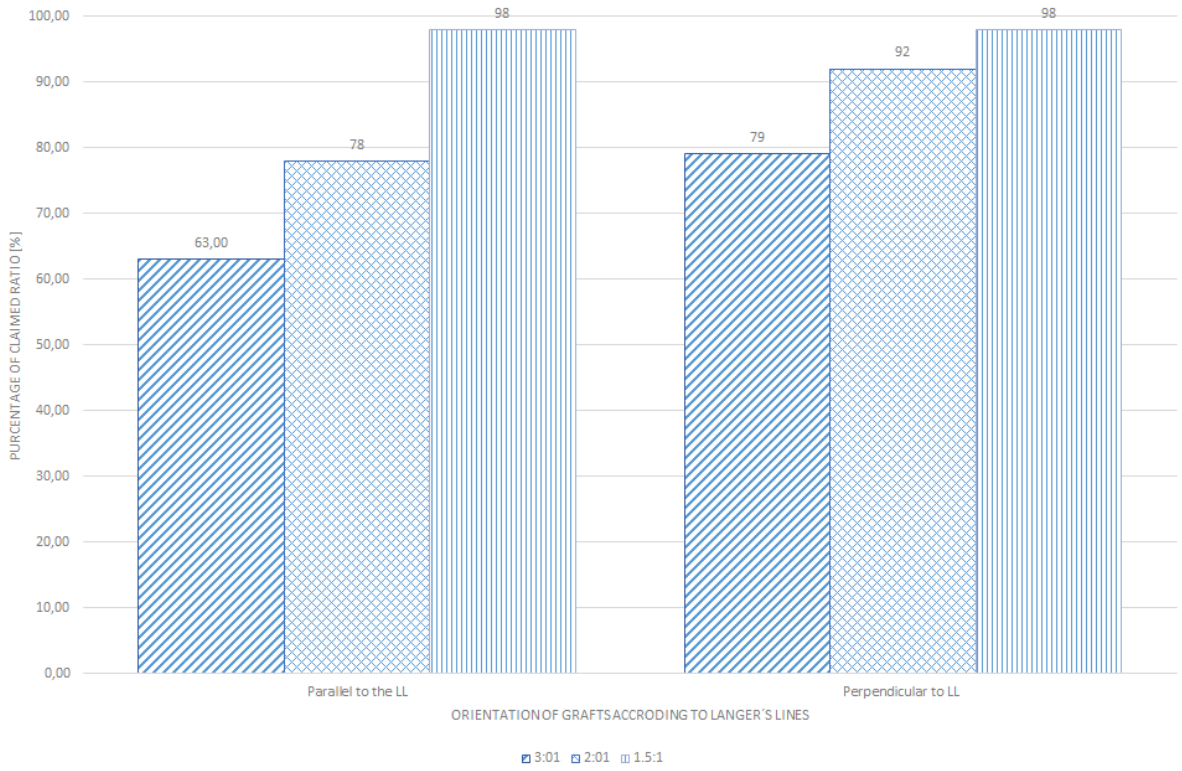

Fig.6,

View publication stats